

The density cavitons generated by interactions of plasma with a moving body in its wake region in space

SHANJUN MA^{1,2} and XIAOQING LI³

¹Purple Mountain Observatory, Academia Sinica, Nanjing 210008, P. R. China

²Department of Physics, Jiang Xi Normal University, Nanchang 330027, P. R. China

³Department of Physics, Nanjing Normal University, Nanjing 210008, P. R. China

(Received 24 June 2001)

Abstract. Numerical calculations are performed based on a set of equations that describe the non-steady, nonlinear interactions between a moving body in space and plasma. The results show that density cavitons and potential solitons are formed owing to modulational instability if the envelope of the high-frequency modulational field is sufficiently intense.

1. Introduction

When a conducting body moves through the ionosphere at mesothermal speeds, complicated interactions occur between the moving body and the plasma around it. Since many artificial vehicles have entered outer space, great interest has arisen in the study of the effects of the interactions. Many experimental investigations (Cairns and Gurnett 1991; Enloe et al. 1997; Keller et al. 1997) and theoretical studies (Liu 1969; Gurevich et al. 1969; Al'pert 1983; Li 1989; Biasca and Wang 1995; Hastings 1995; Dobrowolny 1998) have been devoted to the effects in the vicinity of a body moving through the ionosphere. In early theoretical studies, non-steady-state interaction was not considered for the purpose of simplicity. This is a serious shortcoming. In the last 10 years or so, some works, including several observations from space shuttle missions (Cairns and Gurnett 1991; Biasca and Wang 1995; Enloe et al. 1997; Dobrowolny 1998) have concerned the problems of current–voltage characteristics of a charged probe and density distribution in the plasma wake. Through an analysis of the momentum equation of the plasma electrons, Dobrowolny (1998) derived a result that appears to be consistent with recently acquired data on the current–voltage characteristics from missions with tethered satellite systems when parameters were properly chosen. In low Earth orbit, Enloe et al. (1997) obtained the current collection behavior from flight experiments on charging hazards and wake studies using a highly negatively biased probe that was placed in a plasma wake. Using a particle-in-cell (PIC) code, Biasca et al. (1995) also investigated current collection of a highly negatively biased probe in the wake region. However, they put emphasis on the influence of the current–voltage characteristics for different axial probe positions and probe potentials.

To study the problems arising from the interactions between a moving body and a plasma, investigators usually use the steady and linear method to treat the interactions. Few of them introduce non-steady-state and nonlinear problems into their studies. However, it is well known that a conducting body moving in the ionosphere can excite plasma waves and plasma instabilities. In fact, a large-amplitude solitary wave has been observed (Bakai et al. 1977). Since plasma waves and plasma instabilities are typically non-steady-state and nonlinear problems, it is important to consider non-steady-state and nonlinear effects in their study. On the other hand, many vehicles have a 'stealth' characteristic that prevents them from being detected by radar. However the density cavitons generated by the interactions of plasma with vehicles cannot be concealed. 'Stealth' vehicles can be traced by detecting the motion of the density cavitons if one knows the characteristic of the density cavitons.

Since the characteristic dimension of a body moving in the ionosphere, which is usually the order of one or a few meters, is much smaller than the mean free path $L(L > 10^2 \text{ m})$ of the particles, kinetic theory can be used to describe the processes in the vicinity of a moving body. If the velocity of body V_0 is mesothermal which means that $V_{T_i} \ll V_0 \ll V_{T_e}$ (where V_{T_i} and V_{T_e} are the thermal velocities of electrons and ions respectively), the equilibrium of electrons is very weakly disturbed by the body, i.e. kinetic effects for electrons can be neglected. Hence, we can use the hydrodynamical equations for electron description, and the ion distribution function f_i should obey the Vlasov equation. In addition, the quasineutral approximation is valid because the directed kinetic energy is much larger than the electrostatic potential energy due to the electric field effect, and in many of ionospheric dynamic problems of interest, the geomagnetic field effect is negligible (Liu 1969).

The interactions between a moving body in space and its highly rarefied plasma environment are one of the basic problems in space plasma physics. A set of non-steady, nonlinear equations that describe the interactions for the far wake in a self-consistent manner was obtained by Li (1989). In this work, due to the complexity of the equations, the effect of the ponderomotive force and the linear modulational instability of a finite envelope have been discussed, although the effect of interaction between a moving body and plasma also appears in the equations. Now, in this paper, the coupling equations are solved numerically in the derivation of the nonlinear evolution of modulational instability. At the same time, the pattern of density cavitons is obtained.

This paper is organized as follow: In Sec. 2, based on the fluid equations for electrons and the Boltzmann equation for ions, we obtain the non-steady-state, nonlinear coupling equations that describe the interaction between a body in space and the plasma in its wake. In Sec. 3 the non-steady-state and nonlinear coupling equations are solved numerically in two dimensions with three field components. Finally, Sec. 4 presents a discussion and conclusions.

2. Non-steady-state and nonlinear coupling equations

First, we write the essential steps in the derivation of the non-steady, nonlinear coupling equations between the envelope of a high-frequency field and density disturbance, which were obtained by Li (1989). The fluid equations for electrons and

the Maxwell equations can be written as follows:

$$\frac{\partial n_e}{\partial t} + \nabla \cdot (n_e \mathbf{V}_e) = 0, \tag{1}$$

$$\frac{\partial \mathbf{V}_e}{\partial t} + (\mathbf{V}_e \cdot \nabla) \mathbf{V}_e = \frac{e}{m_e} \left(\mathbf{E} + \frac{1}{c} \mathbf{V}_e \times \mathbf{B} \right) - \frac{\gamma_e T_e}{m_e n_e} \nabla n_e, \tag{2}$$

$$\nabla \times \mathbf{E} = -\frac{1}{c} \frac{\partial \mathbf{B}}{\partial t}, \tag{3}$$

$$\nabla \times \mathbf{B} = -\frac{1}{c} \frac{\partial \mathbf{E}}{\partial t} + \frac{4\pi e}{c} (n_e \mathbf{V}_e - n_i \mathbf{V}_i), \tag{4}$$

$$\nabla \cdot \mathbf{B} = 0, \tag{5}$$

where n and \mathbf{V} are the density and velocity respectively, subscripts i and e represent ions and electrons respectively, γ_e is the specific-heat ratio for electrons, and T_e is the temperature of electrons in energy units. The other symbols have their usual meanings.

On the basis of the two-time-scale approximations (Li 1985), all field quantities can be separated into fast-time-scale and slow-time-scale components, and in a natural way we can assume that the average value of the fast time scale over the slow time scale vanishes. In the far-wake region and on a slow time scale, electrons can easily follow ions wherever ions go due to their small mass; so the quasineutrality condition $n_s^e = n_s^i = n_s$ is valid. Finally, we have the amplitude transport equation of the fast-varying field and the low-frequency disturbance equation for the electron density from the above equations as follows (Li 1989):

$$2i\omega_{pe} \frac{\partial}{\partial t} \mathbf{E} + c^2 \nabla \times \nabla \times \mathbf{E} + \frac{\delta n}{n_0} \omega_{pe}^2 \mathbf{E} - \gamma_e V_{Te}^2 \nabla (\nabla \cdot \mathbf{E}) = 0, \tag{6}$$

$$\left(\frac{\partial^2}{\partial t^2} - \gamma_e V_{Te}^2 \nabla^2 \right) \frac{\delta n}{n_0} = \frac{e}{m_e} \nabla^2 \varphi + \frac{1}{m_e} \nabla^2 \left(\frac{|\mathbf{E}|^2}{16\pi n_0} \right), \tag{7}$$

where φ is the low frequency electric potential. In order to obtain (6) and (7), we have introduced a high-frequency modulational field as follows:

$$\mathbf{E}_f = \frac{1}{2} [\mathbf{E}(\mathbf{r}, t) e^{i\omega t} + \text{c.c.}], \tag{8}$$

where the envelope $\mathbf{E}(\mathbf{r}, t)$ is a slowly varying function over time. For transverse plasmons, we have the dispersion relation $\omega^2 = \omega_{pe}^2 + k^2 c^2$, $\omega_{pe} \gg kc$. The group velocity of transverse plasmons is much smaller than the light velocity. This condition is used in (6) and (7). In addition, we have also used the following condition.

$$W = \frac{|\mathbf{E}_f|^2}{4\pi n_0 T_e} \ll 1. \tag{9}$$

For the low-frequency disturbance, we have

$$V_{Ti} \gg \frac{\Omega_0}{k}, \quad \Omega_0 = \Omega + \mathbf{k} \cdot \mathbf{V}_0 \approx \mathbf{k} \cdot \mathbf{V}_0, \tag{10}$$

where Ω is the frequency of the ion disturbance. Considering the above equation, for the subsonic case, the first term on the left-hand side of (7) is much smaller than the second term. So we can neglect it under the condition of a static limit.

Equation (7) becomes

$$\frac{\delta n}{n_0} = -\frac{U_{\text{eff}} + e\varphi}{\gamma_e T_e}, \tag{11}$$

where

$$U_{\text{eff}} = \frac{1}{16\pi n_0} |\mathbf{E}|^2 \tag{12}$$

is the potential resulting from the high-frequency field. Equation (11) shows the Boltzmann distribution of the electrons in the field, which is composed of the ponderomotive force and the electrostatic force. We should note that for the supersonic case, (11) is not valid and we have to use (7) as a main equation.

On the other hand, in order to close (6) and (11), we have to study the influence of the slowly varying field φ on the ion flow. Since the body's velocity is greater than the thermal velocity of the ions, a disturbance of the ions occurs basically because of the interactions between the body and ions. In a coordinate system moving with the body, the collisionless Boltzmann equation for the ion distribution is of the form

$$\frac{\partial f_i}{\partial t} + \mathbf{V} \frac{\partial f_i}{\partial \mathbf{r}} - e_i \frac{\partial \varphi}{\partial \mathbf{r}} \frac{\partial f_i}{\partial \mathbf{p}} = A_i(\mathbf{r}, \mathbf{V}, t) \delta(F), \tag{13}$$

where \mathbf{p} is the momentum of ions, A_i is the interaction function between the body and ions, the surface of the body is determined by the equation $F(\mathbf{r}_s) = 0$, and \mathbf{r}_s is the radius of the body. Using the condition of a low-frequency disturbance (10), the combination of (11) and (13) yields (Li 1989)

$$\frac{\delta n}{n_0} = -\frac{U_{\text{eff}}}{\gamma_e T_e + T_i} + \frac{T_i}{\gamma_e T_e + T_i} Q, \tag{14}$$

$$Q = \frac{V_0^2 \pi R_0^2}{V_{T_i}^2 2\pi z^2} \exp\left(-\frac{|\mathbf{V}_0|^2}{2V_{T_i}^2} \frac{x^2 + y^2}{z^2}\right), \tag{15}$$

where the condition $x \neq 0$ and $y \neq 0$ have been used (Al'pert et al. 1965). Through the substitutions

$$\hat{\mathbf{r}} = \frac{2}{3} \frac{\omega_{pe}}{c_s} \mu \mathbf{r}, \quad \tau = \frac{2}{3} \mu \omega_{pe} t, \quad \hat{\mathbf{E}} = \frac{\sqrt{3}\mathbf{E}}{8\sqrt{\pi n_0 \mu (\gamma_e T_e + T_i)}}, \quad \mu = \frac{m_e}{m_i},$$

$$n = \frac{3}{4\mu} \frac{\delta n}{n_0}, \quad \hat{\mathbf{V}}_0 = \frac{\mathbf{V}_0}{c_s}, \quad \alpha = \frac{c^2}{3V_{T_e}^2}, \quad c_s^2 = \frac{T_e}{m_i}.$$

Equations (6) and (14) can be written as (Li 1989)

$$i \frac{\partial}{\partial t} \hat{\mathbf{E}} + \alpha \nabla \times \nabla \times \hat{\mathbf{E}} - \nabla(\nabla \cdot \hat{\mathbf{E}}) + n \hat{\mathbf{E}} = 0, \tag{16}$$

$$n = -|\hat{\mathbf{E}}|^2 - \frac{3}{4\mu} \frac{T_e}{\gamma_e T_e + T_i} |\hat{\mathbf{V}}_0|^2 \frac{\pi \hat{R}_0^2}{2\pi \hat{z}^2} \exp\left(-\frac{T_e}{2T_i} |\hat{\mathbf{V}}_0|^2 \frac{x^2 + y^2}{z^2}\right). \tag{17}$$

Equations (16) and (17) describe the nonlinear coupling of interest to us between the high-frequency field and density disturbance. Equations (16) and (17) are only valid in the far-wake region under the condition of interaction $W < 1$. In (17), the last term on the right-hand side is the effect of low-frequency potential, which comes from the interaction between the moving body and ions. When a body with velocity \mathbf{V}_0 that is much larger than the thermal velocity of ions moves, there is

a change in the ion distribution behind the body. This change produces a low-frequency electric potential. The influence of the electric potential is reflected in this non-standard term.

3. Numerical results

The coupling equations (16) and (17) can be solved numerically in two dimensions with three field components under the condition of a finite-amplitude transverse wave. The purpose of the choice enables us to calculate all the field quantities with the numerical simulation method. We use two dimensional FTCS (time forward-difference and space central-difference method) as the numerical method. Meanwhile, the natural boundary conditions in the r direction, i.e. the field quantities are zero when $\hat{r} \rightarrow \infty$, are used in the numerical simulations. In the z direction in the calculation, a periodic boundary condition has been used. In a cylindrical coordinate system, the initial condition is chosen as

$$\begin{aligned} \hat{E}(\hat{\mathbf{r}}, \tau = 0) = & -\frac{E_0}{\hat{r}} i \frac{2\pi}{\hat{z}_0} \sin\left(\frac{2\pi\hat{r}}{\hat{r}_0}\right) \tanh\left(\frac{\hat{r}}{\hat{r}_0}\right) \exp\left(i\frac{2\pi\hat{z}}{\hat{z}_0}\right) \mathbf{e}_r \\ & + \frac{E_0}{\hat{r}} \frac{2\pi}{\hat{z}_0} \sin\left(\frac{2\pi\hat{z}}{\hat{z}_0}\right) \sin\left(\frac{2\pi\hat{r}}{\hat{r}_0}\right) \exp\left(i\frac{2\pi\hat{z}}{\hat{z}_0}\right) \mathbf{e}_\varphi \\ & + \frac{E_0}{\hat{r}} \left[\frac{2\pi}{\hat{r}_0} \cos\left(\frac{2\pi\hat{r}}{\hat{r}_0}\right) \tanh\left(\frac{\hat{r}}{\hat{r}_0}\right) \right. \\ & \left. + \frac{1}{\hat{r}_0} \sin\left(\frac{2\pi\hat{r}}{\hat{r}_0}\right) \operatorname{sech}^2\left(\frac{\hat{r}}{\hat{r}_0}\right) \right] \exp\left(i\frac{2\pi\hat{z}}{\hat{z}_0}\right) \mathbf{e}_z, \end{aligned} \quad (18)$$

Equation (18) represents a very slowly varying vector field (Zakharov 1984), and has the form of traveling transverse wavepacket. The amplitude of the high-frequency electric field radiated by an antenna has the form of a wavepacket. Although (18) is not the same as the real electric field, it enables us to get more realistic results because it has a similar form to the real electric field. In addition, the choice of an initial wave field (18) can shorten the time of field collapse. On the other hand, because the field has the property of axisymmetry, the initial condition should be axisymmetric. Here, the case $r = 0$ should be excluded. In fact, (15) is obtained under the condition $r \neq 0$, i.e. $x \neq 0$ and $y \neq 0$ in Cartesian coordinates (Al’pert et al. 1965; Li 1989). The choice of the initial condition (18) is based on the consideration of these facts. In (18), $\hat{z}_0 = 50$ and $\hat{r}_0 = 25$ are the widths of the wavepacket of the electric field. The initial condition satisfies the condition for a transverse wave, $\nabla \cdot \hat{\mathbf{E}}(\hat{\mathbf{r}}, \tau = 0) = 0$, and has $|\hat{\mathbf{E}}|_{\max}^2(\tau = 0) = 2.99$. The spatial range of the numerical simulation is chosen as $\Delta\hat{z} = 50$ and $\Delta\hat{r} = 25$. Their dimensional values are $\Delta z \approx 40$ m and $\Delta r \approx 20$ m. The dimensionless distance between the back surface of the moving body and the simulation space is $\hat{L}_0 = 15$, which corresponds to a dimensional value of about $L_0 = 12$ m. The parameters of the moving body and the ionosphere are chosen as $V_0 = 10^6$ cm s⁻¹, $R_0 = 100$ cm, $n_e = 10^5$ cm⁻³, and $T_e = 3000$ K (Al’pert et al. 1965). From the electron temperature, it is easy to obtain the parameter $\alpha = 6.6 \times 10^5$ in (16). The evolution of the solution of (16) and (17) with the initial condition (18) is shown in Fig. 1. In Fig. 1, we have used the expressions $\tau = \tau_n$ with $\delta\tau$, step $\delta\tau = 0.000005$ and the dimensionless quantity $W = |\mathbf{E}_f|^2/4\pi n_0 T_e$ defined in (9), with $n = \delta n/n_0$.

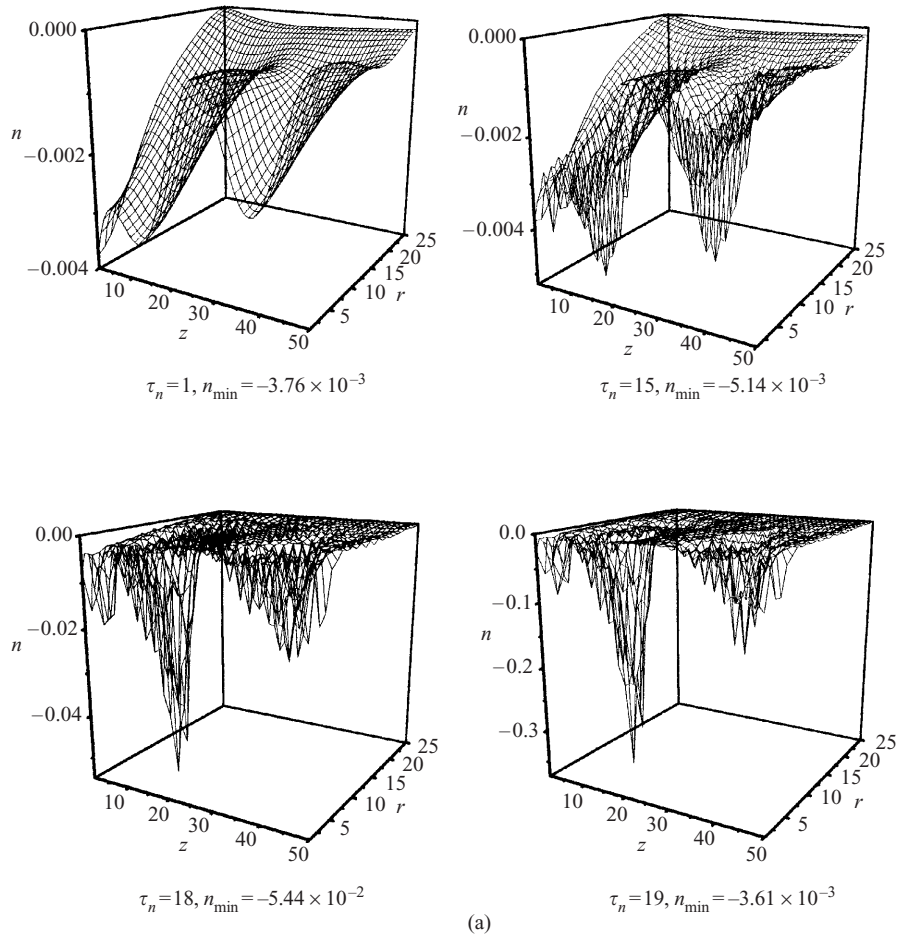


Figure 1. For caption see facing page.

4. Discussion and conclusions

From Fig. 1(b), we can see that the collapses result in the formation of an electromagnetic soliton and the growth rate of the perturbation is proportional to the electric field. This conclusion is qualitatively the same as the analytical prediction of Li (1989). The distributions of the collapses of electric field and density cavities are shown in the figure. This distribution indicates that the growth rate of the perturbation in the whole space of the numerical simulation is different and the growth rates at the peaks of collapse and the density cavities are larger.

In (17), the first term of the density disturbance on the right-hand side comes from the ponderomotive force of the high-frequency field in the static limit. This term indicates that the maximum disturbance of the density occurs at the location where the intensity of the field is maximum. Meanwhile, (17) shows us that the maximum value of the non-standard term is at the origin of the simulation region and the values of other points that are away from this point decline rapidly. From Fig. 1(a), we know that the effect of the non-standard term near the origin is at first larger than the ponderomotive force term. With increasing time, the influence of the ponderomotive force becomes more and more important. Figure 1(a) also

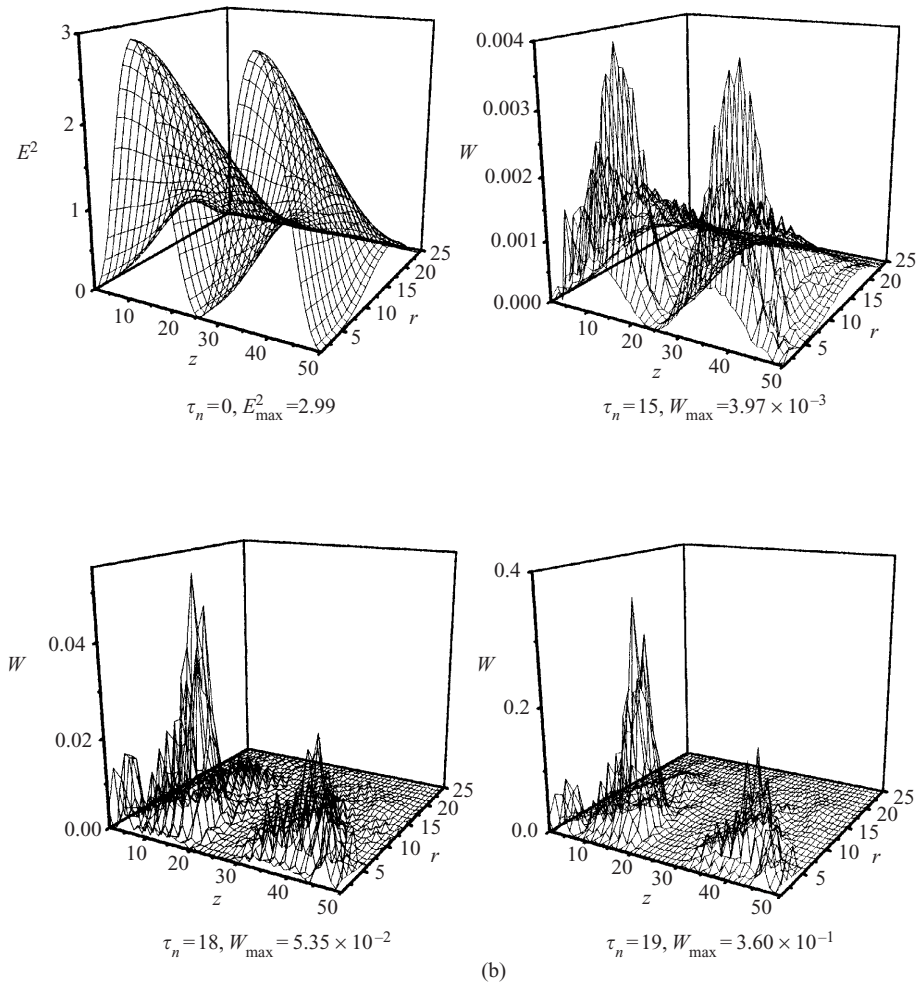


Figure 1. Collapse evolution contours of density $\delta n/n_0$ (a) and electric field $W = |\mathbf{E}_f|^2/4\pi n_0 T_e$ (b).

tell us that the collapses of the field result in the formation of density cavitons in the far-wake region. This is very useful, since the density cavitons can reveal the trace of a ‘stealth’ vehicle. We can find the vehicle by detecting of the density cavitons.

It can be seen from (16) that the density disturbance, the intensity of the field and the derivative of the field can influence the collapse pattern. First, from Fig. 1(a) we know that the most important part of the density disturbance comes from the non-standard term. Although the value of the non-standard term is small and the initial distribution of the electric field is determined by the initial condition, the change in the derivative of the electric field produced by non-standard term is very important. It can determine that the collapses are more likely start to occur near the origin. Of course, this change contains the combined effect of the non-standard term and the initial electric field. However, non-standard term is more important for the formation of the collapse pattern. Figure 1(b) also proves this point.

The numerical results show that the envelope field itself suffers collapse, leading to localization of the field. This means that when time increases, the intensity of field becomes stronger and stronger, and the range of the field is smaller and smaller at the locations of collapse peaks. However, we should note that the numerical calculation does not go on for ever. When the evolution time is larger than a certain value, the field collapses rapidly. This leads to the formation of a very strong field in which the condition $W < 1$ is not valid. This particular value of the evolution time corresponds to $\tau_n = 19$ in our calculation, and we stop our calculation there. In addition, when $W > 1$, stronger turbulent interactions occur between field and particles. The field energy will be transferred to the particles through the interactions. Since the particle energy (i.e. $k_B T_e$) increases and the field energy decreases, W will decrease until the condition $W < 1$ is satisfied again. The time of the stronger turbulent interactions, compared with the weaker interaction, is very short. We do not at present know the physical evolution process during the very short period.

Finally, we indicate that for a transverse plasma wave, because its group velocity is much smaller than the velocity of light, it is not easy for it to escape from the source region. This enables the wave to collapse through interactions between the wave and the particles. On the other hand, considering the above discussion, the choice of initial condition (18) is not unique. The amplitude of any propagating transverse wave that is a slowly varying function of time can be chosen as the initial condition if it satisfies the condition for a transverse wave. Different initial conditions may lead to different locations of the collapse peaks (different collapse patterns). The collapse velocity may be different – fast or slow. However, the collapse tendency of the envelope field is similar. In addition, although the main conclusions can be given in a two-dimensional subspace, the numerical simulations that are obtained in three dimensions with three field components are more realistic than the above results. However, it is very difficult to realize the simulation in a three-dimensional space due to the great quantity of calculation required.

From the above studies, we arrive at the following conclusions:

- (i) The motion of a body with antenna system in the ionosphere may directly excite electromagnetic solitons via modulational instability. The numerical results agree with the observed results quoted by Bakai et al. (1977).
- (ii) The density disturbance in the far wake represents also a kind of soliton of evacuation, i.e. a density caviton, if the radiation from the antenna as a pump wave source is sufficiently intense. From the distributions of the density caviton, we can trace the moving body by observing the structure and intensity of the density caviton in the far wake, although the body may be a ‘stealth’ vehicle.

Acknowledgements

S. Ma would like to thank the Natural Science Foundation of Jiang Xi Province for financial support. X. Li would like to thank the National Natural Science Foundation of China for financial support.

References

- Al’pert, Ya. 1983 *The Near-Earth and Interplanetary Plasma*. Cambridge University Press.
 Al’pert, Ya., Gurevich, A. V. and Pitaevskii, L. P. 1965 *Space Physics with Artificial Satellites*. New York: Plenum Press.

- Bakai, A. S., Kuperov, L. P. and Solodovnikov, G. K. 1977 *Sov. J. Plasma Phys.* **3**, 572.
- Biasca, R. and Wang, J. 1995 *Phys. Plasmas* **2**, 280.
- Cairns, I. H. and Gurnett, D. A. 1991 *J. Geophys. Res.* **96**, 13 913.
- Dobrowolny, M. 1998 *Nuovo Cim.* **21**, 85.
- Enloe, C. L., Cooke, D. L., Pakula, W. A., Violet, M. D., Hardy, D. A., Chaplin, C. B., Kirkwood, R. K., Tautz, M. F., Bonito, N., Roth, C., Courtney, G., Davis, V. A., Mandell, M. J., Hastings, D. E., Shaw, G. B., Giffin, G. and Segal, R. M. 1997 *J. Geophys. Res.* **102**, 425.
- Gurevich, A. V., Pitaevskii, L. P. and Smirnova, V. V. 1969 *Space Sci. Rev.* **9**, 805.
- Hastings, D. E. 1995 *J. Geophys. Res.* **100**, 14 457.
- Keller, A. E., Gurnett, D. A., Kurth, W. S., Yuan, Y. and Bhattacharjee, A. 1997 *Planet. Space Sci.* **45**, 201.
- Li, X. Q. 1985 *Astrophys. Space Sci.* **112**, 13.
- Li, X. Q. 1989 *Astrophys. Space Sci.* **153**, 311.
- Liu, V. C. 1969 *Space Sci. Rev.* **9**, 423.
- Zakharov, V. E. 1984 Collapse and self-focusing of Langmuir waves. In: *Basic Plasma Physics II* (ed. A. A. Galeev and R. N. Sudan). Amsterdam: North-Holland, p. 81.